Conference Paper, Published Version

Neelima, Ch.; Sannasiraj, S. A.

Wind Wave Variability In Indian Ocean During South-West Monsoon

Proceedings of ninth International Conference on Hydro-Science and Engineering (ICHE 2010), IIT Madras, Chennai, India.
2 - 5 August 2010

WIND WAVE VARIABILITY IN INDIAN OCEAN DURING SOUTH-WEST MONSOON

Ch. Neelima and **S.A. Sannasiraj***

Abstract: *Wind-waves are of prime importance for many of the offshore and coastal activities. The understanding of wave characteristics in different regions is valuable. In this study, the variability of kinetic energy of wind and waves thus formed has been presented during a typical south-west monsoon period with reference to our Indian coast. A broad classification of Indian Ocean into Southern Indian Ocean, Arabian sea and Bay of Bengal has been made. The wind-wave model WaveWatch III (Tolman, 1999) has been setup over the domain, 30°E – 120°E and 30°N – 50°S and hind casting of waves were made using NCEP wind in a grid resolution of 1.25° x 1.0°. The variability of wind and waves during the period of May to September 2001 has been established. The wave prediction has been compared with buoy data. The wind and wave kinetic energies over the three sub-domains have been established for each month. The variation of wave distribution over the south-west monsoon period has been plotted.*

Keywords: *WaveWatch III, Wave height, Wind and Kinetic Wave energies, Indian Ocean.*

1.0 INTRODUCTION

It is well understood that the knowledge of ocean waves and their variability in its distribution over the ocean basins is of prime importance for any maritime activity. This is of great importance for dictating the optimum ship routing to the choice of locating a time window for installation of an offshore structure. The importance of prediction of the offshore wave environment accelerated in the sixties which laid foundations for the first generation wave model. The challenging task then was the formulation of the momentum transfer from wind to sea surface. These models were incomplete without non-linear wave-wave interactions and the high frequency spectral tail was prescribed. The second generation models evolved about a decade later with the inclusion of non-linear wave-wave interaction terms but not in a full sense. It was due to the lack of computational power in early eighties as well as the difficult task in the integration of non-linear interaction terms. The second generation models were unable to predict complex wind-seas generated by rapidly changing wind fields due to hurricanes, intense, small-scale cyclones or fronts. The models also encountered basic difficulties in treating the transition between wind-sea and swell. The shortcomings in the second generation models were eradicated in the third generation models. The two-dimensional wave spectrum was allowed to grow without any imposed conditions. The formulation of wind-wave momentum transfer was better defined by Snyder *et al*. (1981) and Janssen [1989]. Hasselmann and Hasselmann (1985) formulated discrete integral approximation scheme to evaluate the complex integration of non-linear wave-wave interaction terms. The integration of the non-linear interaction terms are still the time

*Department of Ocean Engineering, Indian Institute of Technology Madras,
Chennai 600 036, India. Email: sasraj@iitm.ac.in*

expensive part of the wave vital role in operational wave predictions. Presently, WAM (The WAMDI group, 1989) and WaveWatch III (Tolman, 1999) are widely used operational third generation wave models in most of the meteorological stations worldwide.

With the state-of-the art wave models, the wave hind casting and forecasting over different regions of world oceans are being established. The understanding of short- and long-term variability of distribution of waves over the defined region of interest is significant. In the present study, the variability of wind waves over the Indian Ocean during a typical south-west monsoon period has been described.

2.0 WIND-WAVE MODELLING

WaveWatch III (Tolman, 1999) is a full-spectral third generation wind-wave model developed at NOAA/NCEP in the spirit of the WAM model (Komen *et al*., 1994). Furthermore, with model version 3.14, WAVEWATCH III (WW-III) is evolving from a wave model in to a wave modeling framework, which allows for easy development of additional physical and numerical approaches to wave modeling. WW-III solves the random phase spectral action density balance equation for wave number-direction spectra. The implicit assumption of this equation is that properties of medium (water depth and current) as well as the wave field itself vary on time and space scales that are much larger than the variation scales of a single wave.

2.1 Physical features of the WW-III

WW-III estimates the wave growth and decay due to the action of wind, nonlinear resonant interactions, dissipation, bottom friction, surf-breaking and scattering due to wave bottom interactions by solving the equations of refraction and straining of the wave field due to temporal and spatial variations of the mean water depth and of the mean current (tides, surges etc.), when applicable. The energy balance equation for the spectrum N(k,θ;x,t) is given as,

$$\frac{\partial N(k,\theta;x,t)}{\partial t}+C_g\nabla_x N(f,\theta;x,t)=\frac{S}{\sigma} \quad (1)$$

The net source term, S defined for the energy spectra is generally considered to consist of three parts, a wind-wave interaction term, S_{in}, a nonlinear wave-wave interactions term, S_{nl} and a dissipation term, S_{ds}. In shallow water, additional processes like, wave-bottom interaction, S_{bot}, depth-induced breaking, S_{db} and triad wave-wave interaction, S_{tr} have to be considered.

The model includes several alleviation methods for the Garden Sprinkler Effect (Booij and Holthuijsen, 1987, Tolman, 2002c), sub-grid representation of unresolved islands (Tolman 2002e), dynamically updated ice coverage. Spectral partitioning is also available for post-processing of point output, or for the entire wave model grid using the Vincent and Soille (1991) algorithm (Hanson and Jenssen, 2004; Hanson *et al* , 2006, 2009).

2.2 Model setup and validation

A third generation wave model, WW-III has been setup over Indian Ocean spanning from 30° E to 120°E and, from 50°S to 30°N with a grid spacing of 1.25° and 1.0°, respectively. ETOPO2 has been used to map the bathymetry in the model domain. The re-analysed global NCEP wind data (Kalnayet al., 1996) for the period from May 2001 to September 2001 in the grid resolution of 1.25° x 1.0° has been extracted and adopted . The NCEP winds were compared with buoy measured wind in Arabian Sea.

There are 4222 sea points. The propagation time step and the source time step are selected as 1 hour and 5 minutes. The wave spectrum is discretized into 15 equidistant directions and in 25 frequencies ranging from 0.0412 to 0.4056 Hz. The wave prediction was compared with wave height measurements at four buoy stations, off Goa (DS1), off Mangalore (DS2), off Kochi (SW3) and off Lakshadweep islands (SW4) in Arabian Sea. These wave observations were obtained from National Data Buoy Program (NDBP) of India. Two buoys are positioned at deep waters (DS1 and DS2) and the other two buoys (SW3 and SW4) are located in relatively shallow waters. Table 1 presents the location of these buoys. The wave model outputs such as significant wave height (H_s), mean wave period (T) and mean wave direction (θ) were obtained at three hourly intervals at the nearest grid points of the buoy locations and then, interpolated to the buoy station. Fig. 1 presents the comparison of significant wave height (SWH) between buoy observation and model prediction at four buoy stations. The comparison is found to be good. The similar comparison with mean wave period and mean wave direction is also found to be good. In general, due to the smoothened wind vectors, the wave prediction is lower than the actual measurements.

Table 1. Location of data buoys

Buoy	Latitude (°)	Longitude (°)	Depth (m)
DS1	15.48	69.27	2098
DS2	10.67	72.55	975
SW3	15.40	73.755	30
SW4	12.93	74.71	75

The occurrence of SWH is up to 4m for most of the duration except during storm weather for two days in the month of May, severe waves of height more than 7m had occurred at DS1. SWHs greater than 2.5 m during May-September are typical of south-west monsoon wave characteristics. The model underestimates during severe storm period. The wave period and wave direction match, for both buoy and model is very good for all the locations.

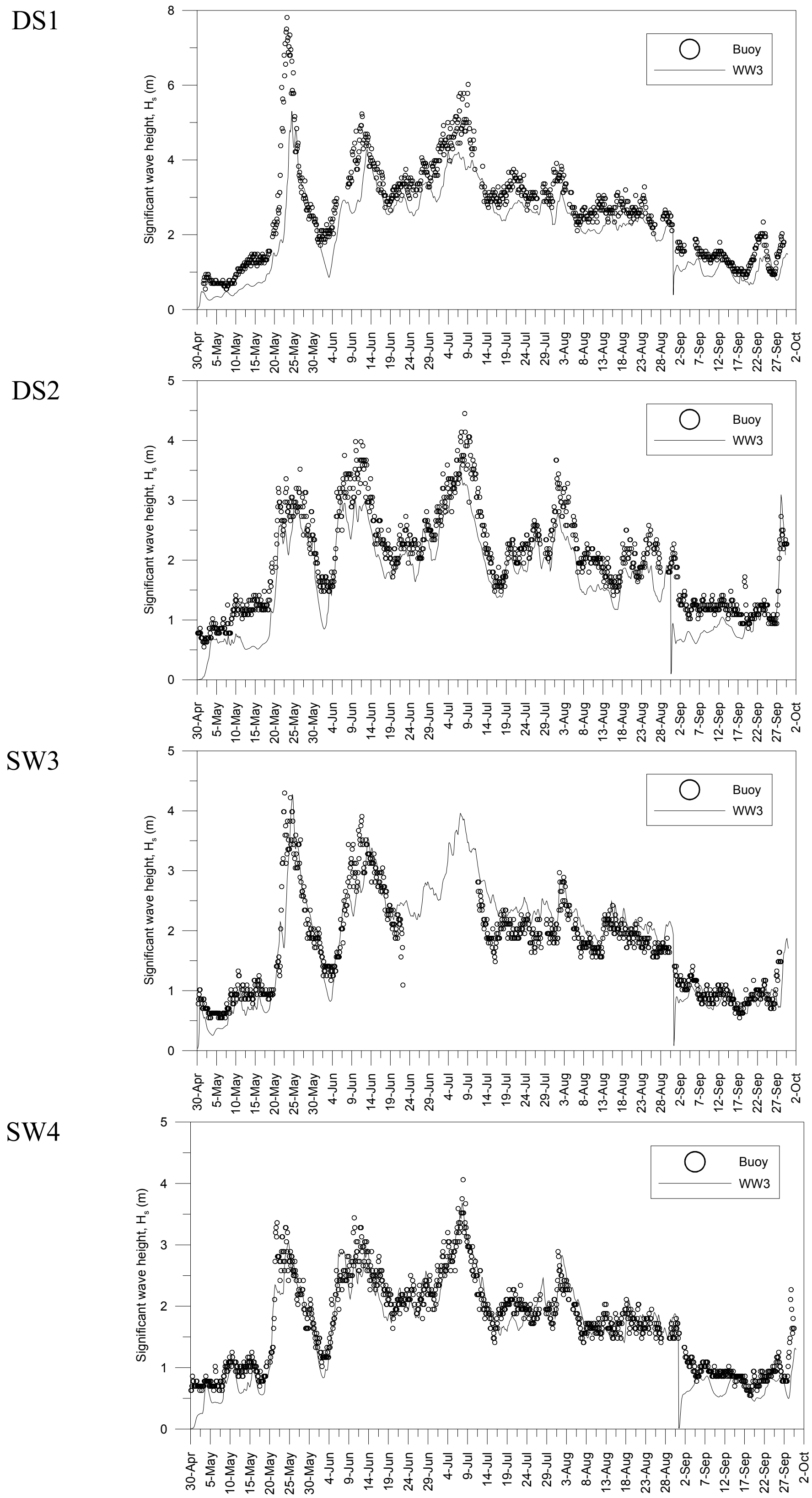

Fig1: Comparison of Buoy observation with Model prediction

3.0 RESULTS AND DISCUSSION

3.1 Wind and Kinetic wave energy distribution

Wind is the mechanical energy input from the atmosphere which is one of the most important sources of energy driving the oceanic general circulation and waves. This energy is transferred to the oceans, mostly through the free surface in the form of momentum transfer mostly through normal stress on the free surface. The estimation of kinetic energy availability in the wind form provides us firsthand information on the possible inducted energy into ocean. Since, the origin of waves is of wind, it has direct correlation with wave formation and its growth.

The space-time history of the atmospheric wind energy in each region, R, and time period, T, can be calculated from,

$$E_A(R,T) = 10\left[\sum_{n\in T}\Delta_t\left(\Delta_s\sum_{i,j\in R}\frac{\rho_a}{2}W_{i,j}^3(t)\right)\right] \quad (2)$$

where, E_A (R,T) is the energy density per unit surface area (J/m^2), ρ_a is the air density, W_{ij}(t) is the wind speed at each space-time grid points, (i, j). The factor 10 is used to take into account the 10-meters boundary layer since the wind speed is measured at 10m above ocean free surface. The inner term under the sum in the above equation is the density of the kinetic energy flux over a surface area, Δ_s for a duration of Δ_t (here, 3 hours=10800sec) which is also the output time step of the model. Summation is done over the specified region, R, and over fixed time period, T. Typical unit of time period is one month. As the wind speed increases, the amount of energy transferred to the sea increases rapidly of the order of third power of wind speed.

The mechanical energy accumulated in wind waves, distributed over space and time, is then calculated by using,

$$E_W(R,T) = \left[\sum_{n\in T}\Delta_t\left(\Delta_s\sum_{i,j\in R}\frac{\rho_w g}{16}H_{i,j}^2(t)\right)\right] \quad (3)$$

where, ρ_w is the water density and H_s is the significant wave height, the model output.

The computation of kinetic energies due to wind and wind-waves has been carried out in three distinct regions in Indian Ocean and these regions are divided into,

(1) Arabian Sea (AS) : 30°E - 65°E ; 0° - 30°N
(2) Bay of Bengal (BoB): 66°E - 120°E ; 0° - 30°N
(3) Southern Indian Ocean (SIO): 30°E - 120°E ; 50°S - 30°N

The computed values of kinetic wind and wind-wave energy for these regions are presented in Table 2 and Table 3, respectively. The distribution per unit surface area has been presented during each months of a typical south-west monsoon period. It can be clearly seen that the kinetic energy of wind and waves is uniformly higher in SIO compared to AS and

BoB. Similar phenomenon for wave energy distribution follows the wind energy distribution and is also of fact that SIO has uninterrupted domain useful for wave growth. Since south-west monsoon is more active in AS, the wind energy distribution is clearly two to three times higher than BoB and the wave energy distribution is nearly 1.5 to 2.5 times more in AS. SIO experiences high concentration of wind and wave energy during these periods.

Table 2. Kinetic energy of wind per unit surface area, E_a (joule/m^2) (*10^{10})

MONTH	AS	BoB	SIO
May	0.6183	0.3575	1.2927
June	1.3434	0.5366	1.4045
July	1.6453	0.5774	1.6930
August	1.1785	0.5598	1.5821
September	1.6472	0.2870	1.3217

Table 3. Wind-wave energy per unit surface area, E_w (joule/m^2) (*10^{10})

MONTH	AS	BoB	SIO
May	0.3599	0.2237	1.3436
June	1.0421	0.4233	1.6015
July	1.2809	0.4890	1.9766
August	0.9372	0.4024	1.6159
September	0.2830	0.1660	1.2305

3.2 Characteristic distribution of waves

To understand the distribution of wave heights during south-west monsoon, the formation of waves has been classified into three regions based on the wave height, as follows:

- Ordinary Waves with SWH <3m
- Severe Waves with 3m < SWH < 6m
- Storm Waves with SWH > 6m

The distribution of waves in Indian Ocean within the limits of less than 3m, 3m to 6m and more than 6m has been shown in Figs.2, 3 and 4, respectively. The contours show the percentage of occurrences of wave height during the south-west monsoon period spanning for five months from May to September 2001. During this monsoon period, it can be noted that severe waves of the order of 3m to 6m had occurred in AS during most of the period but the BoB is relatively calm, except few occurrences on north of BoB. From the model prediction, it is noted that there is no observation on severe stormy waves in AS and BoB, however, the buoy observations show stormy waves during the month of May at DS1. SIO has always been active with moderate to severe waves throughout the five months period studied here.

The biggest waves on the planet are found where strong winds consistently blow in a constant direction. Such a place is found in south of Southern Indian Ocean, at latitudes of -40º to -60º. The waves here occur of an average 7m, with the occasional waves twice that height. The lowest waves occur where wind speeds are lowest, around the equator, particularly where the wind's fetch is limited by islands, However, in these places, the sea water warms up, causing the birth of tropical cyclones. BoB falls under this category, particularly during north-east monsoon period.

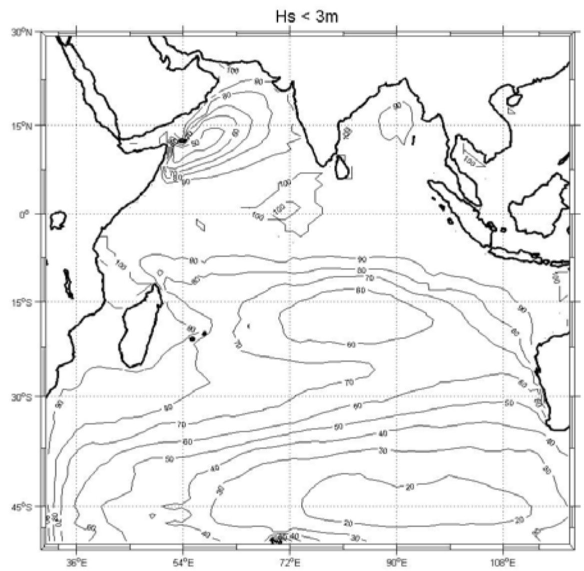

Fig. 2. Distribution of wave heights of less than 3m during south-west monsoon period.

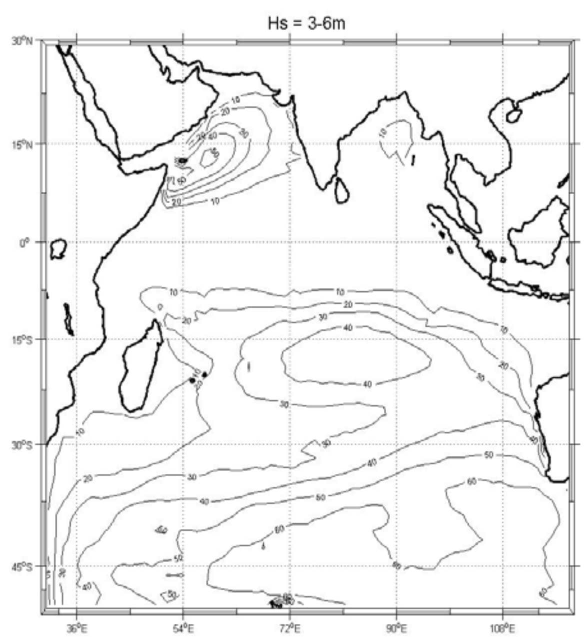

Fig. 3. Distribution of wave heights between 3m to 6m during south-west monsoon period.

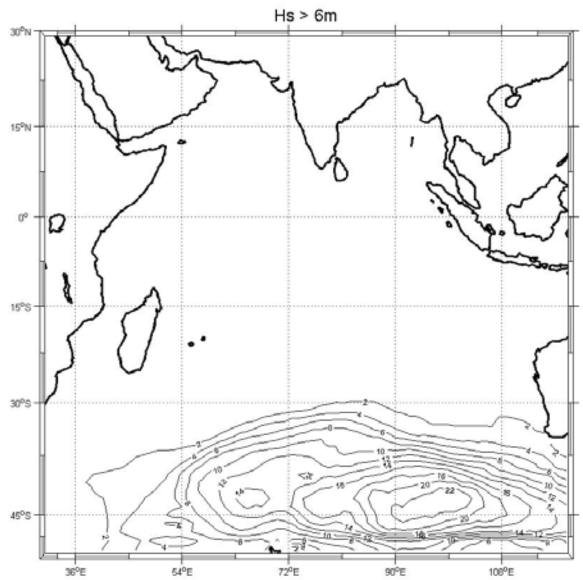

Fig. 4. Distribution of wave heights of greater than 6m during south-west monsoon period.

CONCLUSIONS

The third generation w ind wave model, WaveWatch III has been setup to generate w ind-waves in Indian Ocean during a typical south-west monsoon period. The m odel prediction has been validated with buoy observations at f our stations: off Goa, Kochi, Mangalor e and Lakshadeep islands. The kinetic energy distri bution of wind and the resulting waves shows significant pattern vari ation in Arabian Sea and Bay of Ben gal due to the predominantly south-westerly winds during the study period. The wave activity in BoB is consistently lower compared to AS. However, SIO is always active with the occurrences of stormy waves in the southern most part towards Australia. Further studies to understand the distribution of waves, in particular kinetic energy distribution of wind and waves over Indian Ocean for a period of fifteen years will be carried out.

REFERENCES

Booij, N. and L.H.Holthuijsen, 1987: "Propagation of ocean wave s in discrete spectal wave models", *J.Comput.Physics,* 68, 307-326.

Janssen P.A.E.M., 1989: "Wave induced stress an d the drag of air over sea waves", *J. Phys. Oceanogr.*, 19, 745-754.

Hanson, J. L. and R.E.Jensen, 2004: Wave system diagnostics for numerical wave models, in *8th international workshop on wave hindcasting and forecasting, JCOMM Tech*. Rep, 29, WMO/TD-NO.1319.

Hanson, J. L., and B.A.Tracy, H.L.Tolman and D.Scott, 2006: Pacific hindcast performance evaluation of three numerical wave models, in *9th international workshop on wave hindcasting and forecasting, JCOMM Tech.* Rep.34.Paper A2.

Hasselmann, S., K.Hasselmann, J.H. Allender and T.P. Barnett, 1985: Computations and parameterizations of the nonlinear energy transfer in a gravity-wave spectrum, Part I: A new method for efficient computations of the exact nonlinear transfer integral. *J.Phys. Ocenaogr.,*15, 1369-1377.

Janssen, P.A.E.M., 1989 : Wind-induced stress and the drag of air-flow over sea waves. . *J.Phys. Ocenaogr.,* 19,745-754.

Kalney, E., Kananmitsu, M., Kistler, R., Collins, W., Deaven, D., Gandin, L., Iredell, M.Saha, S., White, G. Woollen, J,Zhu, Y., Chelliah, M., Ebisuzaki, W., Higgins, W., Janowiak, J., Mo, K.C., Ropelewski, C., Warg, J., Leetmma, A., Reynolds, R., Jenne, R., and Joseph, D., (1996). "The NCEP/NCAR reanalysis project", *Bull.Am.Meteorol.Soc.,* 77, 437-471.

Komen G..J., Cavaleri L., Donelan M., Hasselmann K., Hasselmann S. and Janssen P.A.E.M., "*Dynamics and modeling of ocean waves"*, Cambridge university press, New York, (1994).

Snyder R. J., Dobson F.W., Elliott J.A. and Long R.B., 1981: "Array measurements of atmospheric pressure fluctuations above surface gravity waves", *J. Fluid Mech.*, 102, 1-59.

The WAMDI group, 1988 : "The WAM model – a third generation ocean wave prediction model", *J. Phys. Oceanography*, 18, 1775-1810.

Tolman, H.L., 1999 "*User manual and system documentation of WAVEWATCH-III version 3.14"*, Technical Note No. **166**, National Oceanic and Atmospheric Administration, Washington, DC.

Tolman, H.L., 2002c: Limiters in third-generation wind wave models. *The Global Atmosphere and Ocean System*, 8, 67-83.

Vincet, L., and P.Soille, 1991: Watersheds in digital spaces: An efficient algorithm based on immersion simulations, *IEEE Transactions of Pattern Analysis and Machine Intelligence*, 13, 583-598.